Modeling of Biomedical Antennas through Forecasting DNN for the Enlarged Bandwidth

(Article begins on next page)

Modeling of Biomedical Antennas through Forecasting DNN for the Enlarged Bandwidth

Lida Kouhalvandi[1,+], Mohammad Alibakhshikenari[2,△], Patrizia Livreri[3,□],
Ladislau Matekovits[4,* # ◇], Ildiko Peter[5,♣]

[+] *Department of Electrical and Electronics Engineering, Dogus University, Istanbul, Turkey*
[△] *Department of Signal Theory and Communications, Universidad Carlos III de Madrid, Leganés, 28911 Madrid, Spain*
[□] *Department of Engineering, University of Palermo, Palermo, 90128 Sicily, Italy*
[*] *Department of Electronics and Telecommunications, Politecnico di Torino, Turin, Italy*
[#] *Department of Measurements and Optical Electronics, Politehnica University Timisoara, Timisoara, Romania*
[◇] *Istituto di Elettronica e di Ingegneria dell'Informazione e delle Telecomunicazioni, National Research Council, Turin, Italy*
[♣] *Faculty of Engineering and Information Technology,*
University of Medicine, Pharmacy, Science and Technology "George Emil Palade", Târgu-Mureş, Romania

lida.kouhalvandi@ieee.org[1], mohammad.alibakhshikenari@uc3m.es[2], patrizia.livreri@unipa.it[3],
ladislau.matekovits@polito.it[4], ildiko.peter@umfst.ro[5]

***Abstract*—Recently, wireless medical technologies are growing day-by-day resulting in complex structures and topologies. Hence, advanced methods are required for designing and optimizing biomedical devices subject to high-dimensional parameter space. This paper is devoted to presenting an effective approach for estimating frequency responses of an implanted, multiple-input multiple-output (MIMO) antenna through the deep neural network (DNN) in terms of S_{11}, S_{12}, and total active reflection coefficient (TARC) specifications. This impressive approach aims to facilitate the time-consuming simulations in large multi-frequency bands and concurrently reduce the dependency on the designer's experience. All the process is performed in an automated environment and the proposed method is verified by designing and optimizing an implanted MIMO antenna operating in frequency bands of 4.34-4.61 GHz, and 5.86-6.64 GHz. In this design, the Long Short-Term Memory (LSTM)-based DNN is trained for the frequency band between 3-5.8 GHz, and afterward the constructed DNN is employed for predicting the various antenna specifications for the future bandwidth of 5.8-8 GHz.**

***Index Terms*—Bandwidth, biomedical, deep neural network (DNN), extended bandwidth, forecasting, implanted antenna, multiple-input multiple-output (MIMO) antenna, long short-term memory (LSTM).**

I. INTRODUCTION

Implantable medical devices such as biomedical antennas are potentially used for monitoring patients and diagnosing various diseases [1], [2]. These devices capture and transmit data collected from inside the body, referring to the biological state of tissues and organs [3]. Recently, significant advancements have been made in designing and optimizing implantable systems.

In [4], an implantable antenna is designed that operates at the Industrial, Scientific, and Medical (ISM) frequency band; its structure includes an unsymmetrical dipole with a rectangular ground plane and a side-fed radiator. A wearable circularly polarized (CP) antenna is designed in [5] that includes a crossed dipole, a metasurface plane, and a CP feeding network. An implanted antenna operating in ultra-wide bandwidth (from 1.42 GHz to 6.8 GHz) is presented in [6]; its structure has unit cells and cutting flower slots with semicircles on the ground plane. In [7], a medical multiple-input multiple-output (MIMO) water-based implantable antenna is designed and presented. The structure includes minimal metal and no slots in which water is utilized. A miniature implantable antenna with a co-planar feed is presented in [8] operating from 402 MHz to 405 MHz that is compatible with a specific absorption rate (SAR) value. A three-dimensional MIMO antenna operating at 915 and 2450 MHz bands is designed in [9] using a meandered geometry, a high dielectric substrate, and a slotted ground. In [10], a biomedical antenna for the purpose of a leadless pacemaker is designed with the ultra-miniaturized size of 10.66 mm^3. Wireless power transfer (WPT) is an effective approach for implantable medical devices. For this case, in [11] an advanced design consisting of an OFF-body transmitter, a flexible ON-body mu-negative metasurface slab, with an in-body receiver is designed for use in implantable biotelemetric devices. Another implantable MIMO antenna is presented in [12] for the purpose of wireless capsule endoscopy. By reviewing these new and up-to-date references, it can be easily observed that these kinds of devices are high-dimensional, and advanced methodologies are required to achieve targeted specifications. Machine learning techniques with the implementation of neural networks have become a new solution for dealing with the nominated problems [13], [14].

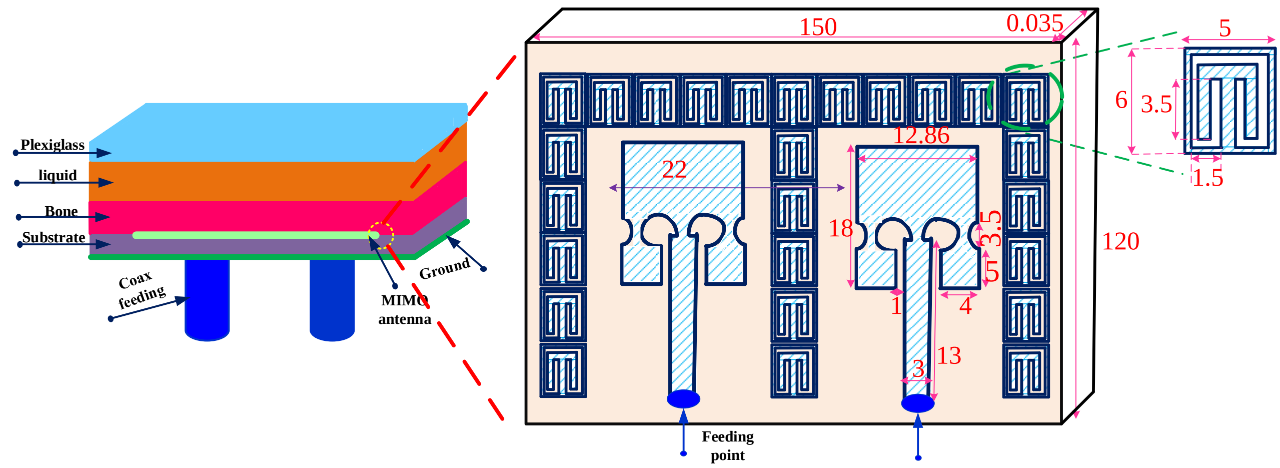

Fig. 1. Structure with the design values in (mm) for the implanted MIMO antenna.

In [15], a machine learning architecture applied for the design of uniform circular arrays is presented; it is a method for reusing angle of arrival estimation models. The deep learning method is employed in [16] leading to predict antenna performance parameters such as resonant frequency, radiation pattern, and directivity with a nominal average root mean square error (RMSE) of 0.0174. In another study, [17] deep learning algorithm is employed for analyzing a dual-polarized high-isolation antenna.

In this paper, we present an effective approach for extrapolating the extended frequency responses of modeled implanted MIMO antenna in terms of S-parameters such as S_{11}, S_{12}, and also TARC specification. This prediction is executed by training the long short-term memory (LSTM)-based deep neural network (DNN) for half of the bandwidth and then the constructed DNN is employed for estimating the remained frequency band. All the optimization process is executed in an automated environment that is created by the combination of numerical tools such as MATLAB and electronic/electromagnetic design automation tools such as Microwave Studio (MS) (Dassault Systèmes). With this methodology, there would be no additional effort for simulating or measuring the whole large frequency bandwidth.

The remained of this work is as follows: Sec. II presents the proposed methodology in a nutshell. Section III is devoted to describing the simulation results achieved from the proposed method. Finally, Sec. IV concludes this paper.

II. Proposed Method

The proposed optimization-oriented algorithm includes designing an implanted MIMO antenna, and afterward, the LSTM-based DNN is trained for extrapolating frequency responses of the modeled antenna at the extended frequency band. All the optimization process is executed automatically by arranging the CPU execution environment, featuring an Intel Core i7-4790 CPU @ 3.60 GHz with 32.0 GB RAM. This section is devoted to describing the proposed methodology that is based on constructing a neural network.

A. *Designing implanted MIMO antenna*

The general structure of implanted MIMO antenna is presented in Fig. 1. For this design, firstly biomedical tissues as 'bone' and 'liquid' are covered by the 'plexiglass' layer and afterwards the MIMO antenna is substituted on the substrate and ground planes. The employed substrate is aluminium oxide (Al_2O_3).

This antenna array consists of two single radiators with a 22 mm distance between them. They are placed on the ground plane with a total size of 150 mm $\times$ 120 mm. The optimal values of design parameters are achieved through genetic algorithm [18]. The surrounded rings around the main single antennas are used for decreasing the surface waves.

B. *Training and constructing LSTM-based DNN for predicting the extended bandwidth*

Figure 2 presents the general structure of the proposed LSTM-based DNN in which the input and output layers represent three specifications as S_{11}, S_{12}, and TARC. The definition of this latter is in terms of the S-parameters and is presented in Eq. (1).

$$TARC = \sqrt{((\mathrm{S}_{11} + \mathrm{S}_{12})^2 + (\mathrm{S}_{21} + \mathrm{S}_{22})^2)/2} \qquad (1)$$

Firstly, the DNN is trained for the first half of the bandwidth and afterwards, the constructed DNN is employed for predicting the behaviour in the remained other half of the bandwidth. This network is trained by the suitable amount of data achieved by iterating the various design parameters and extracting S-parameters and TARC specifications [13]. The hyperparameters of the trained LSTM-based DNN include the number of neurons in the hidden layers. The numbers of neurons and layers are set by the 'rule of thumb' [19].

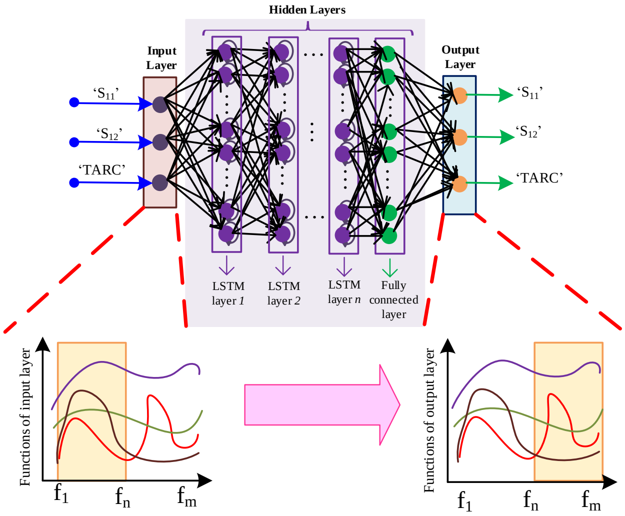

Fig. 2. Proposed DNN for predicting the future extended bandwidth for the designed implanted MIMO antenna.

The accuracy of the LSTM-based DNN is determined by the root mean square error (RMSE).

III. Simulation Results

This section is devoted to presenting the simulation outcomes achieved by designing and modeling the implanted MIMO antenna described in the previous section. Figure 3 presents the S_{11} performance of the designed implanted MIMO antenna in Fig. 1.

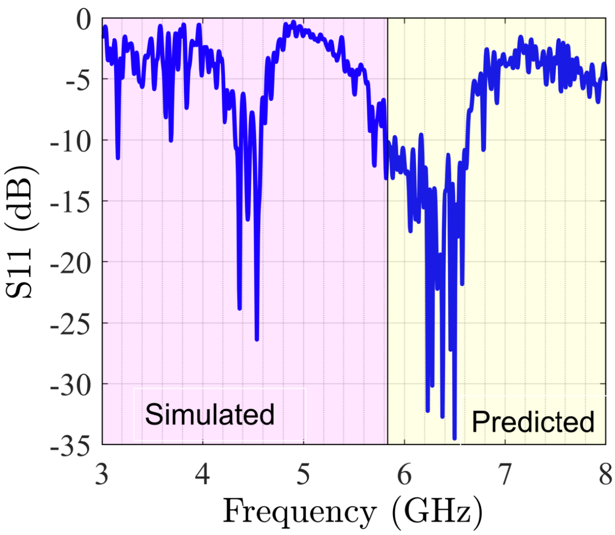

Fig. 3. S_{11} performance of modeled implanted antenna operating in the frequency bands of 4.34-4.61 GHz and 5.86-6.64 GHz.

As it can be observed, it consists of two sections: from 3 GHz up to 5.8 GHz the outcome is achieved by the simulated tool, and from 5.8 GHz up to 8 GHz the S_{11} specification is predicted by the trained LSTM-based DNN. S_{12} and TARC specifications are also presented in Fig. 4 and Fig. 5, respectively that alike to S_{11} result, these figures include simulated and predicated sections for the first half and second half bandwidth. The effectiveness of the trained DNN can be presented by the accuracy factor such as RMSE.

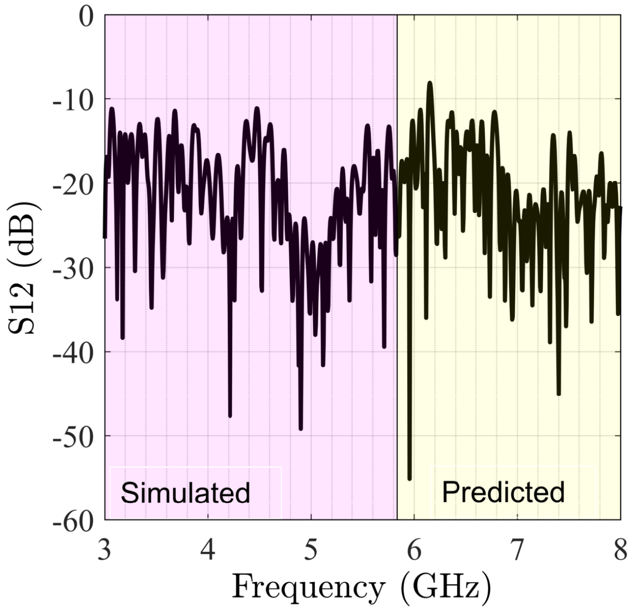

Fig. 4. S_{12} performance of implanted MIMO antenna array.

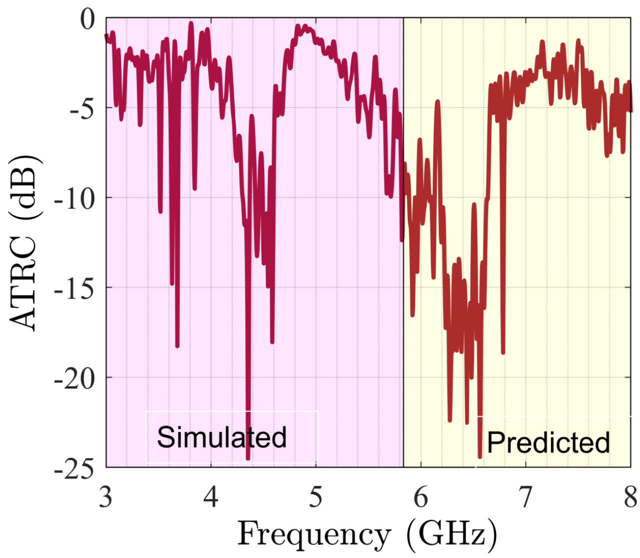

Fig. 5. Representation of TARC specification at the operating frequency band.

Figure 6 shows the normalized RMSE representation for the modeled implanted MIMO antenna that in the 200^{th} neuron, the DNN has 0.018 accuracy. By using the rule of thumb method, the number of hidden layers is determined as 4.

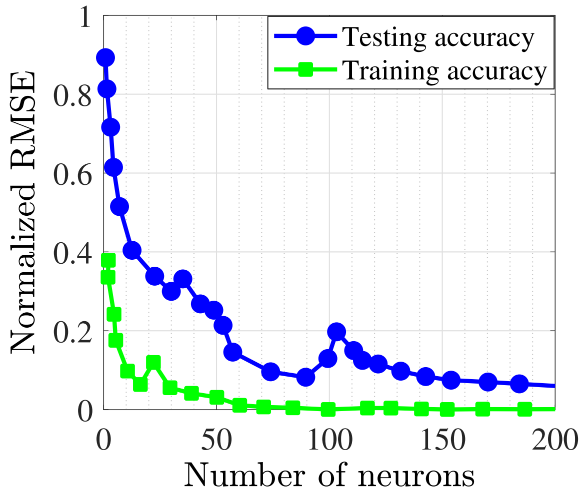

Fig. 6. RMSE value for the trained DNN and modeled implanted antenna presented in Fig. 1.

IV. Conclusion

This paper is devoted to presenting an effective approach for modeling the implanted MIMO antenna in which the performances in the extended bandwidth can be predicted by the constructed LSTM-based DNN. This antenna operates in the frequency band that is essential for the emerging wireless bands. The estimated specifications are in terms of S-parameters (i.e., S_{11} and S_{12}) and of TARC. The proposed methodology results in decreasing the designer's efforts in achieving the full performance of the antenna for the large bandwidth. Here the DNN is firstly trained for the first half of the bandwidth, then the constructed neural network is employed for predicting the outcomes of the next half of the bandwidth. By using this method, the designer's effort in designing, optimizing, and simulating large bandwidth antennas can be reduced considerably.

Acknowledgement

Dr. Mohammad Alibakhshikenari acknowledges support from the CONEX-Plus program funded by Universidad Carlos III de Madrid and the European Union's Horizon 2020 research and innovation program under the Marie Sklodowska-Curie grant agreement No. 801538.

References

[1] M. Qamar, K. Y. Kapusuz, M. A. Thaha, and A. Alomainy, "A compact implantable camera integrated MIMO antenna with polarization diversity for wireless-capsule-endoscopy applications," in *2024 18th European Conference on Antennas and Propagation (EuCAP)*, 2024, pp. 1–5.

[2] A. C. Joshi, J. C. Dash, and D. Sarkar, "Experimental verification of efficiency enhancement of a parasitic patch based wireless power transfer system for IMDs," in *2023 IEEE Microwaves, Antennas, and Propagation Conference (MAPCON)*, 2023, pp. 1–4.

[3] G. Battistini, G. Paolini, A. Costanzo, and D. Masotti, "A novel 3-d printed dual-port rectenna for simultaneous energy harvesting and backscattering of a passively generated uwb pulse," *IEEE Transactions on Microwave Theory and Techniques*, vol. 72, no. 1, pp. 812–821, 2024.

[4] Y. Sui, C. Hou, Y. Wang, K. L. Chung, C. Wei, Z. Li, W.-H. Zong, and J. Wang, "A tissue-independent flexible antenna with miniaturized size for injectable implants," *IEEE Antennas and Wireless Propagation Letters*, vol. 23, no. 3, pp. 945–949, 2024.

[5] K. Zhang, M. Särestöniemi, S. Myllymäki, P. J. Soh, J. Chen, and S. Yan, "A wideband circularly polarized antenna with metasurface plane for biomedical telemetry," *IEEE Antennas and Wireless Propagation Letters*, vol. 23, no. 6, pp. 1879–1883, 2024.

[6] D. Nguyen, Y. Choi, W. Jang, and C. Seo, "An ultra-wide bandwidth with compact size implantable antenna for health monitor microsystem," in *2024 IEEE Wireless Power Technology Conference and Expo (WPTCE)*, 2024, pp. 497–500.

[7] F. Faisal, M. Zada, A. Basir, M. Chaker, and T. Djerafi, "Cost-effective 3d printable water-based mimo and siso antennas for high-data-rate biomedical implantable devices," *IEEE Transactions on Antennas and Propagation*, pp. 1–1, 2024.

[8] R. Kumar and S. Singh, "Cpw-fed conformal PIFA design for implantable iomt devices with wideband performance," *IEEE Sensors Journal*, vol. 24, no. 1, pp. 231–237, 2024.

[9] A. Iqbal, P. R. Sura, A. Smida, M. Al-Hasan, I. B. Mabrouk, and T. A. Denidni, "Dual-band 3-d implantable mimo antenna for IoT-enabled wireless capsule endoscopy," *IEEE Internet of Things Journal*, pp. 1–1, 2024.

[10] F. Faisal, A. Moulay, M. Chaker, and T. Djerafi, "Efficient wireless power transfer to an ultra-miniaturized antenna for future cardiac leadless pacemaker," in *2024 18th European Conference on Antennas and Propagation (EuCAP)*, 2024, pp. 1–4.

[11] I. A. Shah, M. Zada, S. A. A. Shah, A. Basir, and H. Yoo, "Flexible metasurface-coupled efficient wireless power transfer system for implantable devices," *IEEE Transactions on Microwave Theory and Techniques*, vol. 72, no. 4, pp. 2534–2547, 2024.

[12] S. M. A. Shah, M. Zada, J. Nasir, O. Owais, and H. Yoo, "Four-port triple-band implantable MIMO antenna for reliable data telemetry in wireless capsule endoscopy and deep tissue applications," *IEEE Transactions on Antennas and Propagation*, pp. 1–1, 2024.

[13] L. Kouhalvandi, L. Matekovits, and I. Peter, "Key generation of biomedical implanted antennas through artificial neural networks," in *2021 IEEE/ACM Conference on Connected Health: Applications, Systems and Engineering Technologies (CHASE)*, 2021, pp. 161–165.

[14] Z. Wei, Z. Zhou, P. Wang, J. Ren, Y. Yin, G. F. Pedersen, and M. Shen, "Fast and automatic parametric model construction of antenna structures using CNN–LSTM networks," *IEEE Transactions on Antennas and Propagation*, vol. 72, no. 2, pp. 1319–1328, 2024.

[15] G. R. Friedrichs, M. A. Elmansouri, and D. S. Filipovic, "A compact machine learning architecture for wideband amplitude-only direction finding," *IEEE Transactions on Antennas and Propagation*, vol. 70, no. 7, pp. 5189–5198, 2022.

[16] M. R. Khan, C. L. Zekios, S. Bhardwaj, and S. V. Georgakopoulos, "A deep learning convolutional neural network for antenna near-field prediction and surrogate modeling," *IEEE Access*, vol. 12, pp. 39 737–39 747, 2024.

[17] D.-L. Wu, X. J. Hu, J. H. Chen, L. H. Ye, and J.-F. Li, "Ai deep learning optimization for compact dual-polarized high-isolation antenna using backpropagation algorithm," *IEEE Antennas and Wireless Propagation Letters*, vol. 23, no. 2, pp. 898–902, 2024.

[18] H. Cao, X. Duan, J. Wang, Y. Bo, L. Yang, and Q. Wang, "Study of simultaneous transmit and receive phased array based on genetic algorithm," in *2024 IEEE International Conference on Computational Electromagnetics (ICCEM)*, 2024, pp. 1–3.

[19] L. Kouhalvandi, O. Ceylan, and S. Ozoguz, "Automated deep neural learning-based optimization for high performance high power amplifier designs," *IEEE Transactions on Circuits and Systems I: Regular Papers*, vol. 67, no. 12, pp. 4420–4433, 2020.